Journal of Scientific & Industrial Research
Vol. 65, October 2006, pp. 798-807

Experimental adaptive vibration control of smart structures using LVQ neural networks

Rajiv Kumar[1,*], S P Singh[2] and H N Chandrawat[3]

[1]Department of Industrial Engineering, National Institute of Technology, Jalandhar 144 011

[2]Department of Mechanical Engineering, Indian Institute of Technology Delhi, New Delhi 110 016

[3]Department of Mechanical Engineering, Thapar Institute of Engineering & Technology, Patiala 147 001

Received 03 August 2005; accepted 27 June 2006

This paper presents experimental adaptive identification and control of a smart structure featuring piezoceramic-based sensors/actuators. An inverted L-structure with surface bonded piezoceramic sensors/actuators is used for analysis. The state-space presentation, from control input voltages to output sensor voltage is established in multivariable form. It is assumed that the parameters of the smart structure are changing at fast rates. Computational time required for classical identification techniques is generally quite high. For the system, whose parameters change quickly with time, classical system identification techniques fail. So, for improving the system performance, Linear Quadratic Regulator (LQR) cannot be re-designed in real-time for changed parameters of the flexible structure, even if these parameters are identified in real time. Closed loop identification of system parameters and control gains based on system classification technique is proposed for the systems changing at fast rates.

Keywords: Linear Quadratic Regulator (LQR), Neural networks, Piezoceramic-based sensors/actuators

Introduction

With the development of new materials, a trend of using piezoelectric materials as distributed actuators/sensors has emerged. Bailey & Hubbard[1] proposed constant amplitude controller and constant gain controller algorithms for transient vibration control. Crawley & de Luis[2] analyzed the stiffness effect of piezoelectric actuators on the elastic properties of the host structure. Vibration[3] of smart structures by modified independent modal space control was studied by taking the effect of bonding layer between piezoceramic actuators and the host structure. Tzou[4] investigated the piezoelectric effect on the vibration control through a modal shape analysis. Tzes & Yurkowich[5] identified the input-output relation of a flexible single link structure of varying tip mass, instead of modal characteristics for designing the controller, and used Time Varying Transfer Function Estimate (TTFE) algorithm, which updates the frequency component in time domain through Recursive Least Square (RLS) algorithm. Bayard *et al*[6] calculated non-parametric transfer function of the flexible structure in frequency domain, and used curve fitting methods for parametric identification. McGraw[7] used RLS techniques for fitting auto regressive moving average co-efficient to frequency domain data. Milford & Ashokanathan[8] used the same techniques for experimental frequency domain on-line identification and adaptive control of single link flexible structure with time varying tip mass, but using improved methods of signal processing like windowing etc for non-parametric transfer function estimation. Real time adaptive filters[9] for identification of modal parameter for single mode at a time was developed, using input-output data based on infinite impulse response (IIR) filter.

System parameters of the radial drilling machine and SCARA robot change quickly as relative configuration of various arms changes and also affected as payloads are changed. For these situations, computationally intensive methods of parameter estimation cannot be used. Fortunately for these cases, the mode of change of system parameters is known a priori (either by change in relative configuration or by change in payload). System classification techniques based on Learning Vector Quantization (LVQ) methods are quite suitable for these situations. Based on the prior knowledge of the mode of change of system, system parameters, control gains and observer gains are calculated offline for various possible cases. Using LVQ neural networks, all the systems can be

*Author for correspondence
E-mail: rajivsharma1972@yahoo.com

classified into different classes based on supervised learning. In the present study, these systems are classified based on the first few natural frequencies. These natural frequencies can be found from spectrum analyzer in real time. Based on these frequencies, class of the system parameters is found using trained LVQ neural networks. By applying system matrices, control gains and observer gains based on that particular class, system performance can be improved drastically as compared to non-adaptive control.

Mathematical Modeling of Smart Structures

Proposed inverted L-structure (Fig. 1) is mounted with two piezoceramic patches bonded on its surface acting as actuators and two piezoceramic patches bonded on surface acting as sensors.

Finite Element Modeling (FEM)

Lagrange's equation of motion for linear systems is given as

$$\sum_{s=1}^{n}\left[m_{js}\,\ddot{y}_s(t)+c_{js}\,\dot{y}_s+k_{js}\,y_s(t)\right]=Q_j(t)\qquad j=1,2,.....,n \quad \ldots(1)$$

where $y(t)$ is physical displacement, $\dot{y}(t)$ is physical velocity and $\ddot{y}(t)$ is acceleration at time instant 't' for the particular degree of freedom. Also m, c and k are elements of mass, damping and stiffness respectively. Eq. (1) represents a set of n simultaneous second-order ordinary differential equations in generalized coordinates. By this relation, infinitely many degree of freedom distributed system is approximated by an n degree of freedom system. This relation can be written in matrix form as

$$M\,\ddot{y}(t)+C\,\dot{y}(t)+K\,y(t)=Q(t) \quad \ldots(2)$$

where M, C and K are the global mass, damping and stiffness matrices respectively, and $Q(t)$ is the vector of physical applied forces at various degrees of freedom on instant of time t. The column vector $\mathbf{y}(t)$ is the nodal (also called physical) displacements at time t. Using these global mass and stiffness matrices, frequencies and mode shapes of the system can be obtained by modal analysis.

State Space Modeling

For the system having 'r' modes, the system dynamics can be written in matrix state space form as

$$\dot{\mathcal{W}}(t)=\mathcal{F}\,\mathcal{W}(t)+\mathcal{G}u(t)$$
$$y(t)=\mathcal{H}\,\mathcal{W}(t) \quad \ldots(3)$$

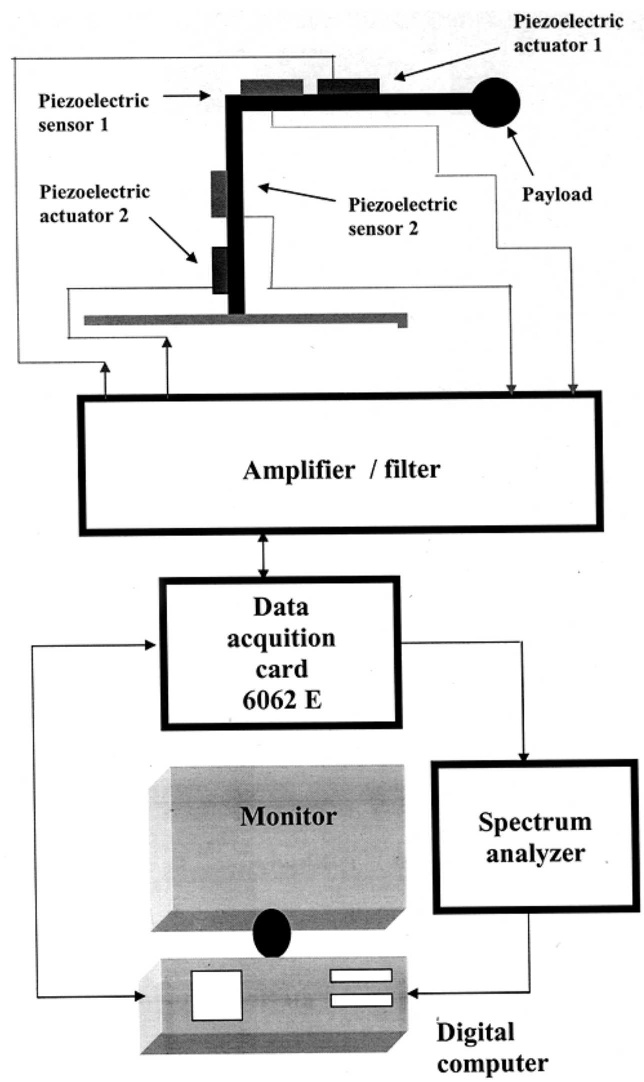

Fig. 1 — Inverted L structure along with experimental setup

where the modal state vector is defined as

$$\mathcal{W}(t)=\begin{bmatrix} w_1(t)\\ w_2(t)\\ w_3(t)\\ w_4(t)\\ \vdots\\ w_{2r-1}(t)\\ w_{2r}(t)\end{bmatrix}$$

Such as $\mathcal{F}$, $\mathcal{G}$ and $\mathcal{H}$ are called system matrices and can be obtained as described by Mierovich[10].

Piezoelectric Sensing and Actuation

When a piezoelectric patch, attached to the distributed structure, is subjected to a change in slope at its two edges, electric charge is developed inside the system. This charge developed in the PZT patch mounted on steel structure[11].

$$\delta(t)=\frac{1}{2}\left(t_s+t_p\right)\left(d_{31}+\upsilon_p d_{32}\right)\frac{E_p}{1-\upsilon_p^2}b\left(\theta_2(t)-\theta_1(t)\right) \quad \ldots(4)$$

where $\theta_2(t)$ and $\theta_1(t)$ are respectively slopes of end 1 and end 2 of PZT patch at the instant of time '*t*'. Thickness of steel and PZT patch are t_s and t_p respectively. Dielectric constants of PZT material are denoted by d_{31} and d_{32}. Breadth of steel beam and piezoelectric patch is denoted by *b*. Young's modulus of elasticity and Poisson's ratio for PZT material are denoted by E_p and υ_p respectively. Similarly, Young's modulus of elasticity (E_s) and Poison's ratio (υ_s) for the steel beam are given in Tables 1 and 2. Voltage developed due to this charge is given by[11],

$$V(t)=\frac{\delta(t)t_p}{\varepsilon_p A_p} \quad \ldots(5)$$

where A_p is the area of PZT patch ε_p is permittivity of PZT material. Since all values except $\theta_1(t)$ and $\theta_2(t)$ are constant in Eq. (4) and (5), Eq. (5) may be written as $V(t)=\Gamma\left(\theta_2(t)-\theta_1(t)\right)$, where Γ is a conversion coefficient.

When a voltage '*V*' is applied across the piezoelectric patch, bending moment 'M_f' of opposite sense, produced at both the edges, is given by[3],

$$M_f=\left[\frac{d31\, b\, E_p\left(E_s t_p t_s+E_s t_b^2\right)}{2\left(E_p t_p+E_s t_s\right)}\right]V \quad \ldots(6)$$

Since all the parameters except V are constant in Eq. (6), subsequent relation may be written as M_f *(Nm)* = Ψ *V* (Volts). Where Ψ is the conversion coefficient.

System Transformations

State space form of system parameters is quite suitable for controller design purposes. The system matrices $\mathcal{F}$, $\mathcal{G}$ and $\mathcal{H}$ are obtained from finite element analysis[10]. However, these matrices form a continuous system. Using the Matlab command c2d, these can be converted into discrete form as

$$\begin{aligned}\dot{X}(k+1)&=A\,X(k)+B\,u(k)\\ y(k)&=C\,X(k)\end{aligned} \quad \ldots(7)$$

Table 1 — Geometrical and mechanical properties

Material property	Steel	PZT
Length of horizontal limb, mm	L_H = 100	—
Length of vertical limb, mm	L_V=100	—
Thickness, mm	t_s=1	t_p=1
Length, mm	l_s=1	l_p=1
Width, mm	B=10	b=10
Young's Modulus, MPa	E_s=210	E_p=64
Density, kg/m^3	ρ_s=7800	ρ_p=7650

Table 2 — Electrical properties of PZT

Property	Symbol	Value
Piezoelectric charge constant, m V^{-1}	d_{31}	$171\text{x}10^{-12}$
Piezoelectric charge constant, m V^{-1}	d_{32}	$171\text{x}10^{-12}$
Poisson's ratio	υ_p	0.28
Permittivity, Fm^{-1}	ε	$106\text{x}10^{-12}$

System Classification using Supervised Learning

System Classification based on Spectral Analysis

The system matrix (*A, B, C*) depends upon systems natural frequencies and mode shapes. As the payload changes from zero to a maximum specified value considered for the system, the systems natural frequencies are changed. So there is direct relationship between tip payload and system matrices. For each payload, the system has distinct natural frequencies. Also with the change in relative configuration of the respective arms of the inverted L-structure, system's natural frequencies are changed. The system parameters are directly related with the natural frequencies. Taking the certain length of the 'on-line' data in time domain and using the spectral analysis techniques, the first two or three natural frequencies can easily be estimated (Fig. 2A). The system parameters are classified offline, based on the first few natural frequencies (Fig. 2B). Similarly, the controller gain matrices and Kalman filter gain matrices are calculated offline for each set of system parameters. Based on these values of natural frequencies, relevant group of the system parameters,

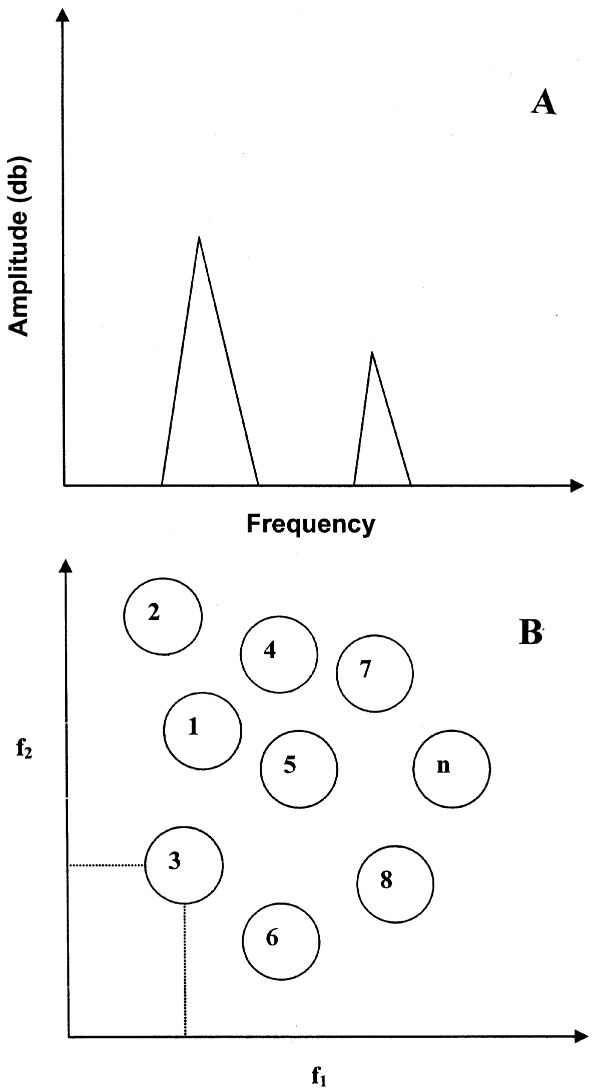

Fig. 2 — System classification based on supervised learning: A) Modal amplitude at different frequencies; B) Classifications based on frequencies

controller gains matrices and Kalman filter gain matrices are identified online.

The first three natural frequencies of the flexible structure for various combination of vertical limb length (VLL), horizontal limb length (HLL) and tip load (TL) are calculated. VLL (74, 85, 95 and 100), HLL (84, 90, 95 and 100) and TL (0-9 g with step of 1 g) form a total of 160 combinations (4 x 4 × 10). The frequencies and mode shapes are calculated using FEM techniques for all the 160 systems. For all the possible combinations of VLL, HLL and PL, first three natural frequencies are never equal (Table 3). At the most, two frequencies match. The third natural frequency varies considerably. Using above equations, system matrices *A, B* and *C* are calculated for each class.

For some different classes, first three natural frequencies are quite nearer to each other. These classes belong to different payloads and different configuration (different HLL and VLL). A unique combination of three frequencies was noticed for a particular class. Not all the three frequencies are equal simultaneously. At the most, two frequencies can be similar, but the third frequency differs. It proves that first three natural frequencies are sufficient to classify any particular class of the system.

Learning Vector Quantization Neural Networks (LVQNN) for System Classification

Using adaptive filters, system parameters can be estimated at fast rates, but are not so accurate for active vibration control applications. Nonlinear optimization techniques give accurate results, but are computational expensive. Other frequency domain online identification techniques are accurate, but control signals generated are not optimal.

By identifying system parameters offline for all possible configurations and using vector quantization techniques, it is possible to categorize system matrices based on natural frequencies. LVQNN can easily classify system parameters for all the different sets based on first three natural frequencies (Fig. 3). Offline computations are required for training of the neural networks (NNs). These trained weights can now be used online, to identify a particular class of the system with certain system matrices, controller gains and observer gains. An excitation signal of small amplitude and containing frequencies (0-600Hz) is continuously applied to the structure.

Implementation of System Classification to Inverted – L Structure

Using 'Neural Network Toolbox' of commercially available software 'MATLAB', implementation of the above technique becomes quite easy. Using commands 'INITLVQ' and 'TRAINLVQ', flow chart (Fig. 4) for the working of LVQNN is executed. Command 'SIMULVQ' is used to simulate the trained NN as follows

The command 'INITLVQ', is used to initiate the network. The syntax of the command is [*W*1, *W*2] = INITLVQ (*P*, S1, *T*). The Inputs used are *P*, S1 and *T* and the outputs are *W1* and *W2*. Where *P* is a (*R* x *Q*) matrix of input vectors, S1=1160 (number of neurons in the hidden layer), *T* is (S2 x *Q*)matrix of target vectors, *W1* is (S1x *R*) weight matrix for competitive

Table 3 — First three natural frequencies at different configurations and tip loads

Length of vertical limb, mm	Length of horizontal limb, mm	Payload g	Natural frequency, Hz			Class number
			I	II	III	
100	100	0	29.14	74.24	362.04	1
95	95	1	29.11	74.91	354.11	52
74	95	4	28.28	79.78	329.62	75
100	90	1	28.77	75.30	369.04	82
95	90	1	30.42	78.51	383.60	92
74	90	4	29.90	82.31	363.41	115
95	84	2	29.51	76.39	395.90	133
74	84	6	28.29	79.02	399.64	157

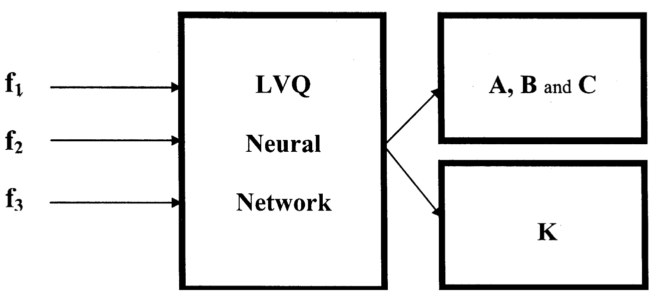

Fig. 3 — Learning vector quantization neural network used as system classifier

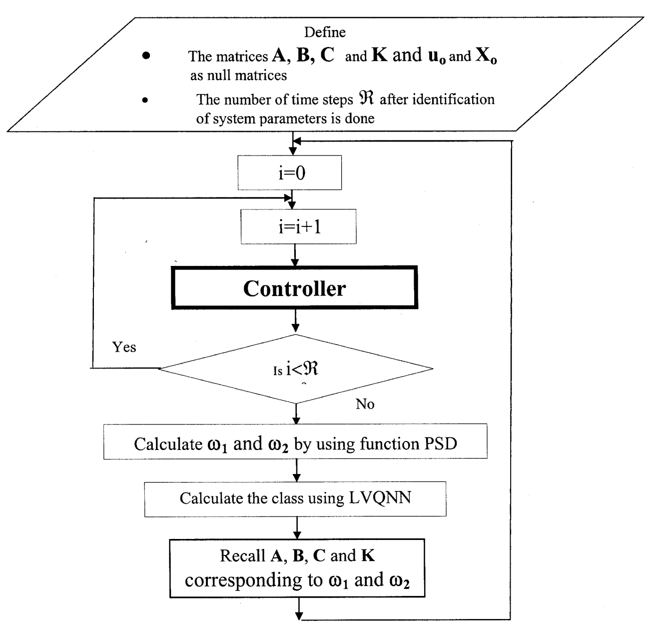

Fig. 4 — Algorithm for real-time identification and adaptive vibration control

layer and *W2* is (S2xS1) weight matrix for linear layer. Also *R*= 3 (number of elements in input vector), *Q*=160 (No. of input vectors to be classified), S2=160 (number of classes to be classified). *W1* and *W2* are chosen by random functions, automatically by the computer. The command 'TRAINLVQ', is used to train the network. The syntax of the command is [*W1'*, *W2'*] = TRAINLVQ (*W1*, *W2*, *P*, *T*, T_P). The Inputs used are *W1*, *W2*, *P*, *T* and T_P and outputs are *W1*', *W2*' i.e. updated values of *W1*, *W2*. Where T_P –Vector of training parameters {number of iterations after which results are to be displayed, total number of iterations, learning constant} which is given as {100 15000 0.014}. These trained weight matrices, *W1*' and *W2*'i, are saved and can be used further for actual classification.The command, 'SIMULVQ', is used to find the class of the system. The syntax of the command is [*A1*, *A2*] = SIMUFF (*P*, *W1'*, *W2'*). The Inputs are *P*, *W1'*, *W2'* and outputs are *A1* and *A2*. Where *P* is a matrix of input (column) vectors; *W1'* is weight matrix for competitive hidden layer, *W2'* is weight matrix for linear output layer. *A1* is the output of the competitive hidden layer and *A2* is the output of the linear output layer. From *A1* and *A2*, the class of the gain matrices can easily be detected.

Although there is certain difference in the natural frequencies obtained from FEM and that obtained experimentally. A wrong system can be classified based on these analytical frequencies. But even the wrong system is so close to the original (actual) system that almost same controller performance can be obtained.

Linear Quadratic Gaussian (LQG) Controller

LQG controller is a combination of Linear Quadratic Regulator (LQR) and Kalman Filter.

Modeling the Noise Characteristics

Two types of noises are considered: (i) Measurement noise (MN); and (ii) Process noise (PN). Measurement and process error has been considered as zero mean. The noise free part of the signal is obtained by repeating the experiment several times for an input sequence and taking the average of that output sequence. In the present case, N = 1024 points are taken to construct one full waveform. The MN vector v (k) is estimates by subtracting the system output from the average output for a particular input sequence. Similar is the case for PN vector w(k).

Full State Feed back Control

LQR with Kalman Filter has proved to be an excellent robust control system design methodology. Using the gain matrix K, control inputs are calculated by the following equation

$$u(k) = -K X(k) \quad \ldots(8)$$

The system matrices A and B and the weighing matrix R and Q are used to calculate the gain matrix K. The relative amplitude of the elements of these matrices determines the amplitude of the control signal vector *u(k)*.

Normally input-output data is available from experimental setup. Due to the presence of MN and PN, the system state and output equations of the stochastic system has the following form

$$X(k+1) = A X(k) + B u(k) + w(k)$$

$$y(k+1) = C X(k) + v(k) \quad \ldots(9)$$

where *v(k)* is the measurement noise vector and *w(k)* is the process noise vector respectively. As assumed *w(k)* and *v(k)* are each zero-mean, white noise sequences in vector form, with known covariance and uncorrelated with each other. Using the inputs *u(k)* and outputs *y(k)*, the future state vector *X(k+1)* can be estimated accurately by using Kalman Filter.

Experimental Setup

In experimental apparatus for vibration control of smart structure (Fig. 1), signals from the PZT patches are fed to the data acquition card. The analog-to-digital conversion and Digital-to-Analog conversion is done through the data acquition card DAQ Card 6062E of National Instruments, having 12 bit resolution for the A/D and D/A conversion. The output range is from –150V to +150V. A low pass filter is applied in the sensing process to avoid interference of higher modes. The Graphics Programming software Lab View is used for experimental implementation. Real Time engine Lab View RT is used to bear the computational burden.

Adaptive Vibration Control

In the present work, a direct approach to give input to the system has been used for optimal accuracy. In this approach, input is taken as the sum of the reference signal and the regulator input. An excitation signal with lower amplitudes i.e. from –20 volt to +20 volt is always applied to excite all the modes for accurate closed loop identification.

Design of Excitation Signal

The input data supplied to the system for system identification should be informative[12]. For the identification of linear systems, there are three basic requirements that govern the choices: a) Asymptotic properties of the estimate (bias and variance) depend only on the input spectrum and not the actual waveform of the input; b) Input must have limited amplitude; and c) Periodic inputs may have certain advantages. Based on several factors, the classification of the input signal can be done into various categories viz. Filtered Gaussian White Noise, Random Binary Signal, Pseudo-Random Binary Signal, Multi Sines and Chirp Signals or Swept Sinusoids. In the present case, to excite the system in closed loop, multisine wave with minimum crest factor[12] and magnitude of the excitation signal near 20 volt is used.

Combined Identification and Control Algorithm

System parameters are estimated based on the newly available data. Then the system matrices and controller is selected and is used for the control of new system to obtain better performance of the control system. The input-output data is transferred from the Lab VIEW real time engine to Pentium II processor and the newly identified system matrices and control gain matrices are transferred from Pentium II processor to the Lab VIEW real time engine through TCP/IP system. Fig. 4 shows the algorithm for online identification and adaptive vibration control. In the present case, to check validity of the proposed technique, first 2 natural frequencies are used to classify the system corresponding to tip loads 0-9 g, for vertical and horizontal limb length of

Table 4 — Comparisons of control parameters for quickly time varying systems by using non-adaptive and adaptive vibration control strategies

Tip load g	Non-adaptive control					Adaptive control					
	Settling time Sec	Modal amplitude, dB				Length of data L	Settling time Sec	Modal amplitude, dB			
		Sensor 1		Sensor 2				Sensor 1		Sensor 2	
		Mode 1	Mode 2	Mode 1	Mode 2			Mode 1	Mode 2	Mode 1	Mode 2
9	2.43	220	58	2000	0	1024	1.45	57	8	460	0
						256	2.10	115	14	995	0
20	5.10	120	3	905	0	1024	3.13	45	0	225	0
						256	3.20	102	7	610	0

100 mm. A LVQNN containing 21 classes for the tip loads from 0-9 g is trained to be used for experimental validation of this technique.

Results and Discussion

Open loop and closed loop responses of the system are obtained experimentally for all the cases (Table 4). This algorithm is quite similar to that for the online identification and adaptive vibration control of slowly time varying systems (Fig. 4). The only difference is that in this case the power spectral density of the data from either sensor1 or sensor 2 is calculated. The natural frequencies of the system are then calculated. These natural frequencies are fed as input to LVQNN. The output of LVQNN will be the identified class. According to this class number, the system matrices A, B, C and the gain matrix K are recalled from the memory, which are stored a priori. The controller again works for $\Re$ number of points without any identification/classification involved. When the iteration counter exceeds $\Re$, identification/classification takes place once again. According to the length $\Re$ of the data points different results were observed as follows:

Data Length is 1024 Points

As the system is excited, the controller designed for 0 g tip load is applied to the system. Data length (1024 point) pertains to a time period of 5 sec corresponding to a sampling rate of 200 Hz. With the non-updated control, a settling time of 2.43 sec is obtained at point B (Fig. 5). The controller starts at point O. At point C, when the 5 sec with respect to point O are completed, the controller stops and updates itself. Now the controller is pertaining to 9 g based on the frequencies obtained from stored data. At the point D, the system is again excited. Since system has been updated, a settling time of 1.45 sec is now obtained. With non- adaptive controller, modal amplitude reduces to 220 dB and 58 dB at sensor1 for the first and second mode respectively. The modal amplitude for the first mode at sensor 2 by non-adaptive controller (NAC) is 2000 dB. Using adaptive controller (AC) modal amplitudes at sensor1 reduce to 57 dB and 8 dB at first and second mode respectively. Similarly, using AC modal, amplitude reduces to 460 dB.

With NAC maximum amplitude of control voltages was 24 volt and 60 volt at actuator no. 1 and 2 respectively (Fig. 6). Using AC, this amplitude raises to 34 volt and 70 volt at actuator no. 1 and 2 respectively. Due to this higher and in phase voltage (with vibrations), settling time decreases. Similarly, the controller is tested for a tip load from 0 g to 20 g. NAC settling time was 4.73 sec. Using AC, this settling time reduces to 3.13 sec. Similarly, with NAC, maximum amplitude of control voltages was 30 volt and 50 volt at actuator no. 1 and 2 respectively. Using AC, this amplitude rises to 35 volt and 68 volt at actuator no. 1 and 2 respectively.

Data Length is 256 Points

In this case, it was observed that the data length of 256 points is sufficient to find accurately the first few natural frequency to the required accuracy. This means that controller updating will now take place after 256/200=1.28 sec. At point O (Fig. 7), the controller starts. At point A, system is excited. From point A to point B, NAC pertaining to 0 g tip load is in action. At point B, controller updating takes place

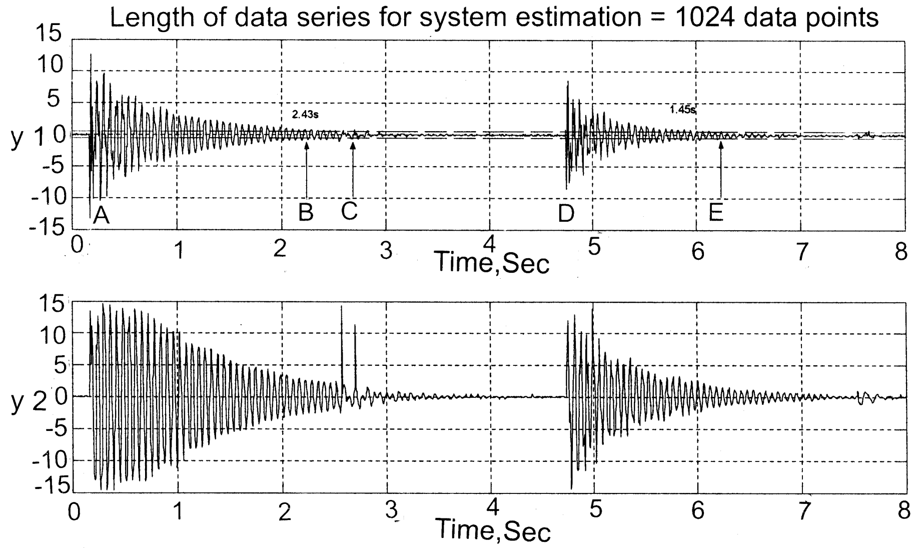

Fig. 5 — Time domain responses by adaptive and non-adaptive control techniques with length of data series as 1024 points

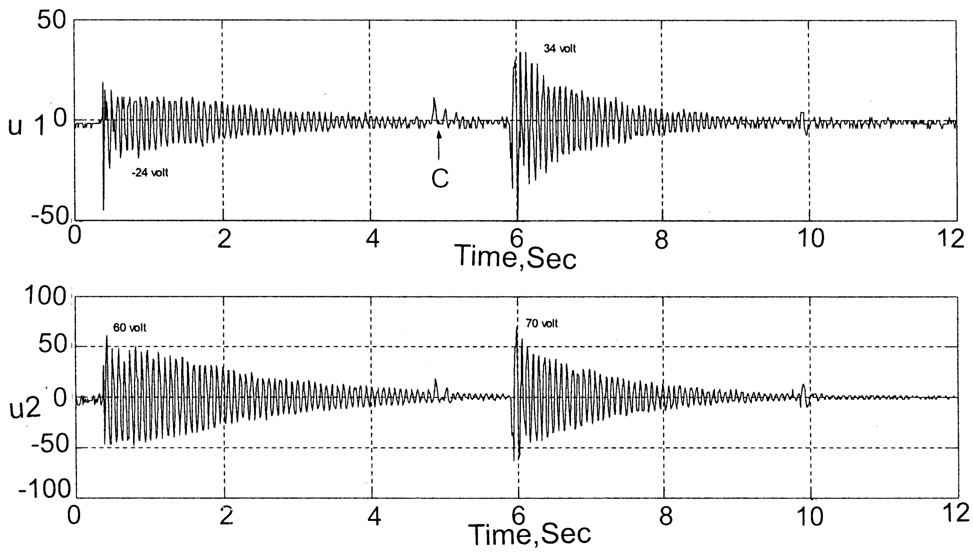

Fig. 6 — Applied actuator voltages by adaptive and non-adaptive control techniques with length of data series as 1024 points

and the system is updated on the basis on the natural frequencies calculated. At point B, the non-updated controller (corresponding to 0 g tip load) stops for few milliseconds and controller updating takes place. At this point, control action pauses for a while, and the structure tends to vibrate freely, causing a sudden shoot up of sensor voltage at point B. The modal amplitude for the first mode at sensor1 reduces to 102 dB instead of 57 dB for 1024 data points. Also the modal amplitude for the first mode at sensor 2 reduces to 610 dB instead of 460 dB for 1024 data points. The reason for this discrepancy is the addition of the affect of first 256 point starting from point A. During this period, NAC was in action, which contributed to some degradation of control properties. Still data length of 256 points is beneficial because, one need not wait for 1024 points of poor performance, and then improves the system for better performance. The controller starts from a peak voltage of 12 volt at actuator no.1 and 50 volt at actuator no. 2 for first 256 points, then controller updates and the control peak voltages shifts to 28 volts at actuator no. 1 and 50 volts at actuator no. 2 (Fig. 8).

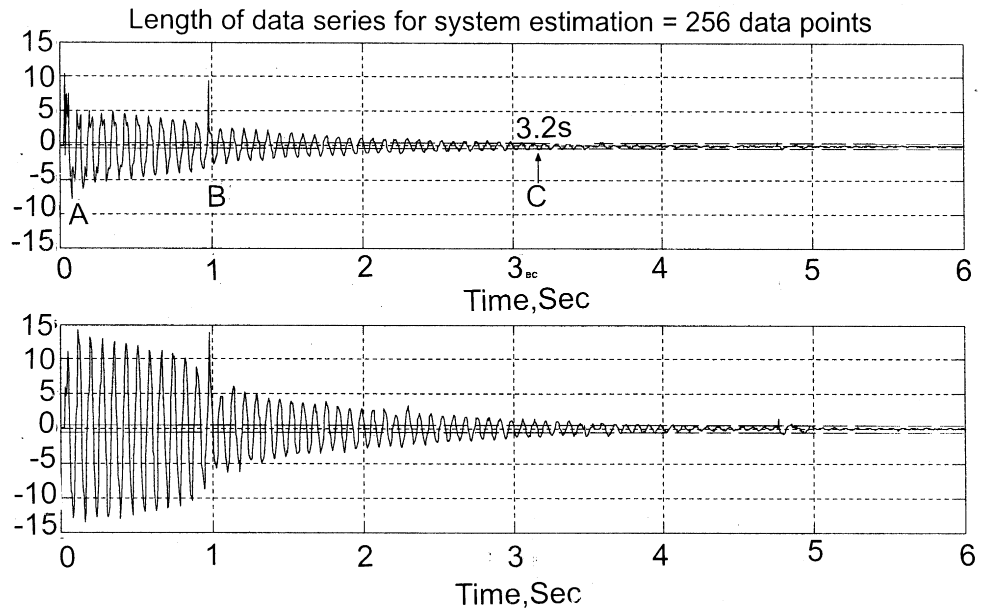

Fig. 7 — Time domain response adaptive and non-adaptive control techniques with length of data series as 256 points

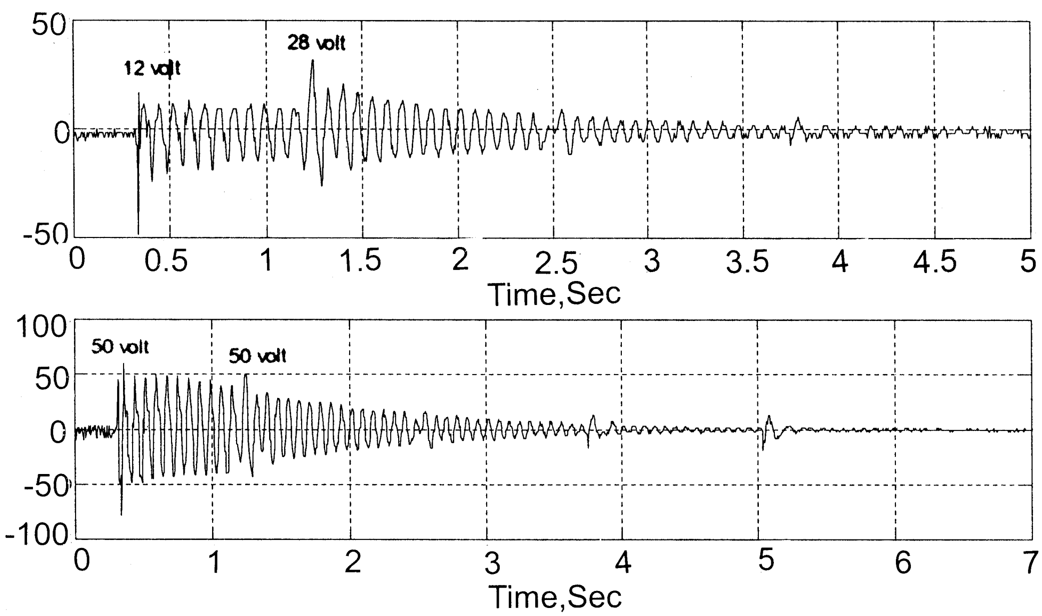

Fig. 8 — Applied actuator voltages by adaptive and non-adaptive control techniques with length of data series as 256 points

By decreasing the length of data series, control performance decreases. For L = 256, settling time increases and modal amplitude reduction decreases. But at the same time, it has advantage of wasting very less time in non-adaptive time intervals. System performance improves rapidly. This may be because at lower value of data length, identification frequency increases. At more number of time instants, identification takes place. During identification part, controller stops. When the controller stops, vibration amplitude suddenly increases. Hence the settling time as well as modal amplitudes remains at higher values.

Conclusions

Smart robotic manipulators and machine structures with multi-modal participation and multiple systems of actuators and sensors are considered for adaptive control in this work. An inverted L-structure is a partial representative of these types of structures. As system parameters are changed, new system parameters, and hence the controller gains can be calculated by solving the Riccatti equation. However, this method is computational intensive and is not suitable for systems changing quickly with time. LVQ neural networks are used to classify the system parameters, controller gains and observer gains based on the natural frequencies of the structural system. By simulating these neural networks, online identification of system parameters and controller gains is made. By using these parameters and gains, better transient performance can be obtained even for systems with quickly changing parameters.

References

1 Bailey T & Hubbard J E, Distributed piezoelectric–polymer active vibration control of a cantilever beam, *Int J Guid, Contr & Dynam*, **8** (1985) 605-611.

2 Crawley E F & de Luis J, Use of piezoelectric actuators as elements of intelligent structures, *AIAA J,* **25** (1987) 1373-1385.

3 Baz A & Poh S, Performance of active control system with piezoelectric actuators, *J Sound & Vibration,* **126** (1988) 327-343.

4 Tzou H S, Distributed modal identification and vibration control of continua: Theory and applications, *J Sound & Vibration*, **113** (1991) 494-499.

5 Tzes A P & Yurkowich S, A Frequency domain identification scheme for flexible structure control, *Int J Dynamic Syst Measure & Control*, **112** (1990) 427-434.

6 Bayard D S, Hadaegh F Y, Yam Y, Scheid R E, Mettler E & Milman M H, Automated on-orbit frequency domain identification for large space structures, *Automatica*, **27** (1991) 931-946.

7 McGraw G A, On-line identification design for a flexible beam laboratory adaptive control experiment, *Int J Control*, **61** (1995) 525-531.

8 Milford R I & Ashokanathan S F, Experimental on-line frequency domain identification and adaptive control of a flexible slewing beam, *Int J Dynamic Syst Measure & Cont,* **118** (1996) 58-65.

9 Lim T W, Chung T Y & Moon S J, Adaptive bang-bang control for the vibration control of structures under earthquakes, *Earthquake Engg & Structural Dynamics*, **32** (1996) 1977-1994.

10 Microvich, *Elements of Vibration Analysis* (McGraw Hill Publishing Company, UK) 1986, 126-136.

11 Buttler R & Vittal Rao, A state space modeling and control method for multivariable smart structural systems *Int J Smart Mat & Struct*, **5** (1996) 386-399.

12 Ljung, *System Identification: Theory for the User* (Prentice Hall PTR, Upper Saddle River N J) 1999, 12-24.